Title

THE KINETICS OF THE HIGH-TEMPERATURE-LOW PRESSURE TUNGSTEN-NITROUS OXIDE REACTION

Author

Poorter, Gerald L. De

Publication Date

1965-05-24

Thesis/dissertation

UCRL-16019

University of California

Ernest O. Lawrence Radiation Laboratory

THE KINETICS OF THE HIGH-TEMPERATURE–LOW PRESSURE TUNGSTEN–NITROUS OXIDE REACTION

Berkeley, California

DISCLAIMER

Research and Development

UCRL-16019

UNIVERSITY OF CALIFORNIA

Lawrence Radiation Laboratory
Berkeley, California

AEC Contract No. W-7405-eng-48

THE KINETICS OF THE HIGH-TEMPERATURE--LOW PRESSURE TUNGSTEN-NITROUS OXIDE REACTION

Gerald L. De Poorter

(Ph. D. Thesis)

May 24, 1965

THE KINETICS OF THE HIGH-TEMPERATURE-LOW PRESSURE TUNGSTEN-NITROUS OXIDE REACTION

Contents

Abstract v

I. Introduction 1

II. Method and Apparatus 2

III. Procedures

A. Calibration Procedures 5

1. Pump speed measurements 5

2. Mass spectrometer calibration 5

3. Mass spectrometer and ionization gauge calibration for nitrous oxide 6

B. Experimental Procedures 8

IV. Materials 12

V. Results 13

VI. Discussion of Results

A. Qualitative Description 23

B. Deduction of a Possible Reaction Mechanism. 24

C. Formation of Tungsten Oxide. 32

D. Estimation of Rate Constants and Activation Energies. 35

VII. Summary 40

Acknowledgments 41

Appendix-Tables of Experimental Data 42

References. 51

THE KINETICS OF THE HIGH-TEMPERATURE–LOW PRESSURE TUNGSTEN–NITROUS OXIDE REACTION

Gerald L. De Poorter

Inorganic Materials Research Division, Lawrence Radiation Laboratory, and Department of Mineral Technology, College of Engineering, University of California, Berkeley, California

May 24, 1965

ABSTRACT

The kinetics of the tungsten–nitrous oxide reaction were studied at temperatures between 2100°K and 2900°K and at gas pressures between 3×10^{-9} and 10^{-6} atm. The reaction was studied under molecular flow conditions by leaking nitrous oxide into an evacuated chamber containing an electrically heated tungsten filament. The decomposition of the nitrous oxide was followed by measuring the partial pressure of nitrous oxide, nitrogen, and molecular oxygen with a mass spectrometer connected into the system. The rate of tungsten oxidation was determined by following the change in the filament resistance as a function of time for constant temperature and pressure. On the basis of the results of other investigations, $WO_2(g)$ was assumed to be the principal oxide formed.

The principal reaction is decomposition of nitrous oxide, which is unaffected by excess nitrogen but greatly reduced by excess oxygen. About one in a thousand nitrous oxide molecules that strike the surface reacts to form $WO_2(g)$ at a tungsten temperature of 2220°K and a nitrous oxide pressure of 10^{-6} atm, whereas at 2735°K and 10^{-8} atm, one in fifty nitrous oxide molecules that strike the surface is converted to $WO_2(g)$. The results of this investigation are consistent with a six-step reaction mechanism involving:

(a) Physical adsorption of the nitrous oxide,

(b) Partial evaporation of the physically adsorbed nitrous oxide,

(c) Decomposition of the physically adsorbed nitrous oxide molecules into nitrogen gas and chemisorbed oxygen atoms,

(d) Reaction of the physically adsorbed nitrous oxide molecules with chemisorbed oxygen atoms, producing molecular nitrogen and oxygen,

(e) Evaporation of the chemisorbed oxygen atoms, and

(f) Reaction of two chemisorbed oxygen atoms with the tungsten, giving $WO_2(g)$.

The decomposition rate of N_2O and the rate of formation of WO_2 both increase with increasing temperature and pressure.

I. INTRODUCTION

The high-temperature reaction between nitrous oxide and tungsten has apparently never been studied, although the reaction is a promising source of information on the kinetics and mechanisms of gas-solid reactions. Because the tungsten oxides are volatile at high temperatures and low pressures of nitrous oxide, the reacting surface is clean of reaction products. For very low gas pressures, the rate of incidence of gas molecules on the reacting surface can be calculated and controlled. Furthermore, the mechanism of the catalytic decomposition of nitrous oxide on platinum filaments has been extensively studied over wide ranges of pressure and temperature; in order for tungsten oxides to form, the nitrous oxide must decompose, and similarities may exist in the decomposition mechanism of nitrous oxide on platinum and tungsten.

In this investigation, the kinetics of the tungsten–nitrous oxide reaction were studied at temperatures between 2100 and 2900°K and at gas pressures between 3×10^{-9} and 10^{-6} atm, with the object of determining the mechanism of the reaction.

II. METHOD AND APPARATUS

For this investigation, tungsten filaments, electrically heated by a stabilized ac power supply, were placed in an evacuated reaction vessel. Nitrous oxide was introduced into the reaction vessel through a leak valve so that the reaction could be studied under flow conditions. Figure 1 illustrates the apparatus.

The reaction vessel is an Inconel cylinder 8 in. in diam and 12 in. high. The removable top holds the gas-inlet valves and the terminals to which are attached molybdenum electrodes for holding the tungsten filaments. A sight port and a pressure gauge are halfway up the side walls at right angles to each other. In order that the entire vessel can be baked, the top, sight port, and pressure gauge are joined to the reaction vessel by gold O-ring seals. The pump outlet is at the bottom of the reaction vessel, and the tube connecting the reaction vessel and the mass spectrometer leaves from the pump outlet tube, between the reaction vessel and the pumping system.

The pressure gauge (Veeco RG 75K Ionization Gauge) is used in conjunction with a vacuum gauge control panel (Veeco RG 21A). This gauge is calibrated for dry nitrogen.

The gas-supply system consists of (a) a two-liter storage flask, (b) pumps and valves for evacuating and filling the storage flask, and (c) means for measuring the pressure in the storage flask and for leaking gas into the reaction vessel. The storage flask is evacuated by a pump (Kinney KC-2), with a cold trap between. The pressure in the flask is measured by either a thermocouple Gauge or a Zimmerli gauge. Depending on the leak rate desired, either a Veeco Throttle Valve or a Veeco Variable Valve is used to control the gas flow.

The pumping system includes a liquid nitrogen cold trap, a water-cooled spiral baffle, a mercury diffusion pump (CVC MHG 180),

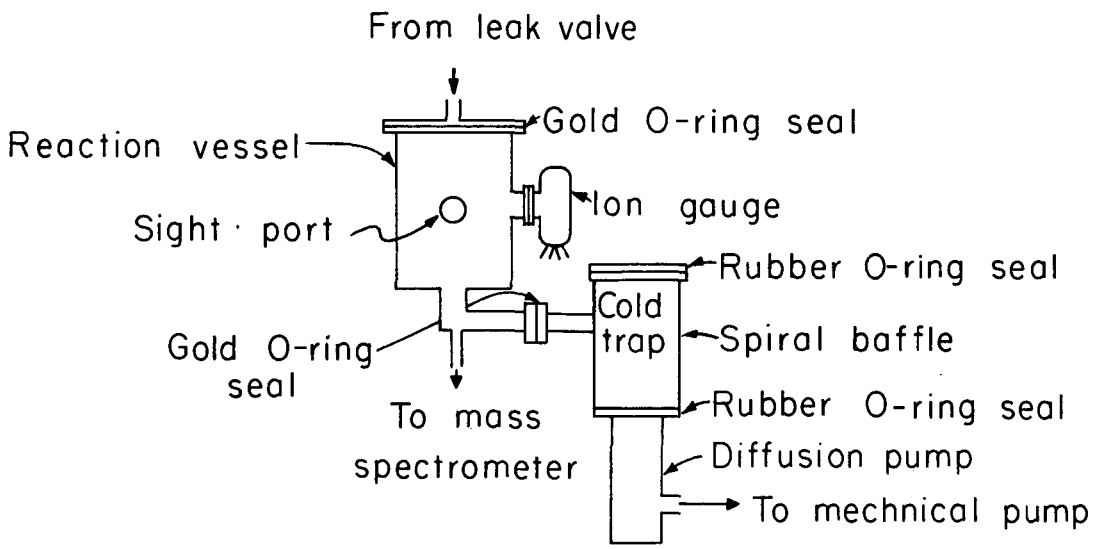

Fig. 1. Sketch of apparatus.

and a mechanical pump (Kinney KC-5). After the reaction vessel is baked overnight by heating tapes, a background pressure of about 6×10^{-10} atm (5×10^{-7} torr) is obtained in the system.

The mass spectrometer used in this investigation is a Consolidated Electrodynamics Corporation Type 21-620. In order to obtain more sensitive measurements, we replaced the molecular leak capsule furnished with the instrument by a flange with a tube leading directly to the reaction vessel. To further increase sensitivity, we placed the mass spectrometer as close as possible to the reaction vessel. The tungsten filament in the cycloid tube was replaced by a rhenium filament, which has better oxidation resistance.

III. PROCEDURES

The experimental procedures of this investigation fall into two groups: those connected with the calibration of the apparatus, and those connected with the collection of data.

A. Calibration Procedures

The calibrations include (a) pump-speed measurements, (b) mass spectrometer calibrations, and (c) mass spectrometer and ionization-gauge calibrations for N_2O.

1. Pump Speed Measurements

The pump speed S is defined by the relationship

$$-\frac{dP}{dt} = \frac{S}{V}(P - P_s),$$

where P_s is the obtainable vacuum, t is time, and V is the volume to be evacuated.[1] In order for us to determine the pump speed, gas is leaked into the reaction vessel until a pressure of about 10^{-6} atm is reached, at which point the gas flow is suddenly stopped and the pressure recorded as a function of time.

If S is independent of P, a plot of log $(P - P_s)$ vs t is a straight line of slope

$$\frac{\Delta \log(P - P_s)}{\Delta t} = \frac{S}{2.303V}.$$

By the use of this method and the volume of the reaction vessel calculated from its dimensions, the pump speed was found to be 12.5 ± 0.5 liters/sec.

2. Mass Spectrometer Calibration

In order for the mass spectrometer to be calibrated, nitrogen is leaked into the reaction vessel until a steady-state pressure is reached. The ion-gauge pressure, which is correct for nitrogen, is

noted and the mass spectrometer output for the 28 peak is recorded. We then plot log peak height or output vs log pressure, and get a straight line. Figure 2 is a typical calibration curve for the mass spectrometer. Since the output of the mass spectrometer was rather unstable, the calibration was checked before or after each experimental run. Thus, the partial pressure of nitrogen in the reaction vessel can be determined from the mass 28 peak height.

3. Mass Spectrometer and Ionization Gauge Calibration for Nitrous Oxide

We used a method reported by Anderson to calibrate the mass spectrometer and ionization gauge for nitrous oxide and oxygen.[2]

The pressure of a given gas measured by the mass spectrometer is proportional to the number of molecules of that gas in the mass spectrometer. Since molecular-flow conditions exist in the tube between the reaction vessel and the cold trap, the number of gas molecules entering the mass spectrometer is proportional to $P/M^{\frac{1}{2}}$, where P is the pressure of the gas in the reaction vessel and M is the molecular weight of the gas. Thus, for a mixture of two gases

$$P_{1(MS)} = k_1 P_1 / M_1^{\frac{1}{2}}$$
$$P_{2(MS)} = k_2 P_2 / M_2^{\frac{1}{2}},$$

where $P_{1(MS)}$ and $P_{2(MS)}$ are the pressures measured by the mass spectrometer, and k_1 and k_2 are constants. If both gases are at the same temperature, $k_1 = k_2$.

According to the kinetic theory of gases,

$$P_1 / P_2 = n_1 / n_2;$$

where n is the mole fraction.

Therefore,

$$P_1/P_2 = P_{1(MS)} M_1^{\frac{1}{2}} / (P_{2(MS)} M_2^{\frac{1}{2}}) = n_1/n_2,$$

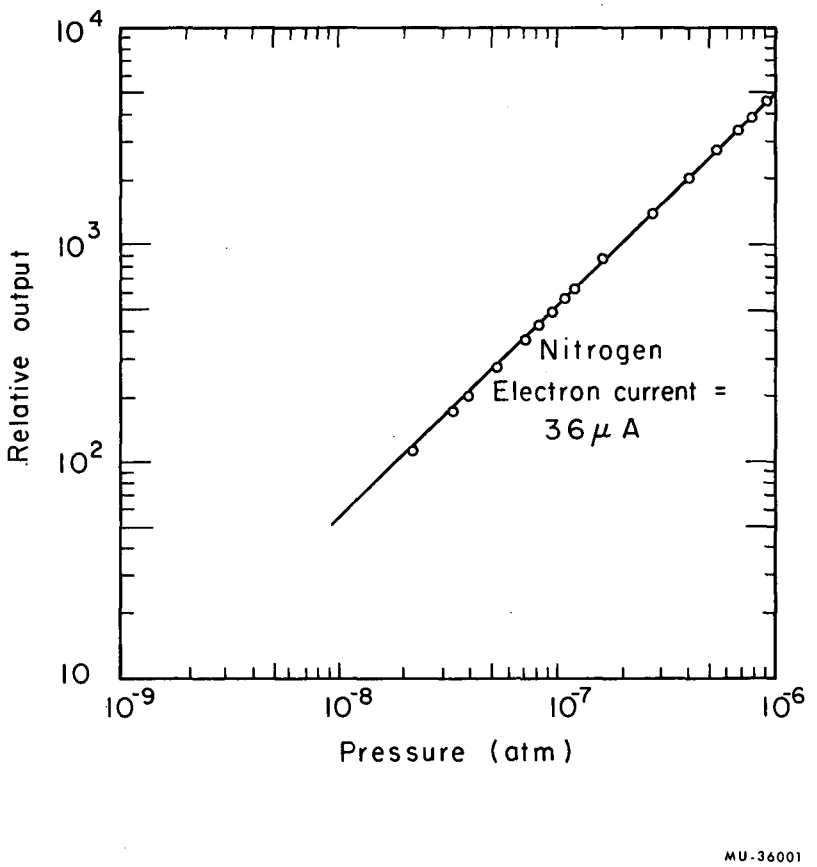

Fig. 2. Typical calibration curve for mass spectrometer.

and

$$P_{2(MS)} = \left(\frac{n_2}{n_1}\right)\left(\frac{M_1}{M_2}\right)^{1/2} P_1(MS).$$

Thus, $P_{2(MS)}$ can be calculated from the results obtained by introducing a mixture for which the relative concentrations of nitrogen and nitrous oxide are known. The constant--by which the pressure read from the nitrogen calibration curve must be multiplied to give the correct pressure for N_2O--was found to be 1.29 ± 0.03 and for oxygen 1.26 ± 0.02.

A knowledge of the mass spectrometer sensitivity and calibration for nitrous oxide allows the ion-gauge sensitivity for nitrous oxide to be easily determined. It was found that P_{N_2O} is $(0.775 \pm 0.015) P_{ion}$.

B. Experimental Procedures

The experimental procedures were designed to provide values for the following parameters:

(a) ϵ, the probability that a N_2O molecule that strikes the filament is removed from the gas phase by decomposition on the tungsten filament (ϵ is not the probability that a N_2O molecule reacts specifically to form tungsten oxide);

(b) R_{44}, the rate of removal of N_2O from the gas phase;

(c) R_{28}, the rate of generation of N_2 from the decomposition of N_2O;

(d) R_{32}, the rate of generation of O_2 from the decomposition of N_2O;

(e) R_w, the rate of loss of tungsten atoms from the filament by reaction.

By definition, the flow rate of gas into the system at the steady state Q is given by

$$Q = SP_o,$$

where S is the pump speed, and P_o is the steady-state pressure with the filament cold. When the filament power is turned on, Q

remains unchanged and the pressure decreases to P, so that the effective pump speed must increase. Therefore

and

$$Q = S'P = SP_o,$$
$$P_o/P = S'/S.$$

The term S' represents the increased pump speed, the increase being caused by the removal of N_2O by decomposition on the filament. Therefore

$$S' = S + \epsilon A_f \nu/n,$$

where ϵ is the reaction probability as defined above, A_f is the area of the filament in cm^2, ν is the number of molecules that strike the filament per cm^2 per sec, and n is the number of gas molecules per liter at P. Thus

$$\frac{P_o}{P} = \frac{S + \epsilon A_f \frac{\nu}{n}}{S} = 1 + \epsilon \frac{A_f}{S} \frac{\nu}{n}$$

and

$$\epsilon = \left(\frac{P_o}{P} - 1\right) \frac{S}{A_f} \left(\frac{\nu}{n}\right)^{-1}.$$

For N_2O at 300°K, n/ν is 0.106, and

$$\epsilon = \left(\frac{P_o}{P} - 1\right) \frac{(0.106)S}{A_f}, \qquad (1)$$

where P_o is the pressure with the filament off and P is the pressure with the filament on; P is the pressure to be used when one is plotting and analyzing the data.

Experimentally, the reaction probability was determined by the following procedure. With the filament off, N_2O was leaked into the system and its pressure was measured with the mass spectrometer.

The filament was then heated quickly to a given temperature and the N_2O pressure was remeasured. From this measurement, the reaction probability was calculated by use of Eq. (1). Then

$$R_{44} = \nu_{44} \epsilon ,$$

where the rate of incidence of gas molecules is calculated at the pressure observed with the filament on.

The rates R_{28} and R_{32} are related to the pressures of nitrogen and oxygen measured in the mass spectrometer. When the rate of arrival at the outlet tube to the mass spectrometer is assumed to be equal to the rate of generation of nitrogen and oxygen at the filament,

$$R_{28} = (\text{const}) P_{28} / A_f (28T)^{\frac{1}{2}}$$

$$R_{32} = (\text{const}) P_{32} / A_f (32T)^{\frac{1}{2}},$$

where T, the absolute temperature of the gas molecules, is assumed to be 300°K, the wall temperature.

The rate of loss of tungsten atoms (R_w), was determined by measuring the change in filament resistance. As derived by Anderson,[3]

$$R_w = \frac{N \rho D L^2}{M A_f} (R_t - R_o) / [(R_t R_o)(\Delta t)]$$

where
- N = Avogadro's number
- ρ = resistivity of tungsten at the temperature of reaction
- D = density of tungsten
- L = filament length
- M = molecular weight of tungsten
- R_t = resistance of the filament at time t
- R_o = initial resistance of the filament
- Δt = time of the reaction.

Filament temperatures were determined from the electrical properties of tungsten tabulated by Jones and Langmuir.[4] End-effect corrections were made as described by Anderson.[5] Before we collected any data, we aged the filaments in oxygen at 10^{-8} atm at about 2600°K for at least 24 h to remove any dissolved carbon as carbon monoxide.

IV. MATERIALS

Nitrous oxide (obtained from the Matheson Company) was advertised as 98.5% pure. The impurities were said to be air, which could not be detected in the mass spectrometer because of the decomposition of the nitrous oxide in the mass spectrometer.

The tungsten, supplied by the Thermionic Products Company, was 99.95% pure. Tungsten filaments 0.010 in. in diam were used. The chemical analysis of the tungsten is given in Table I.

Table I. Analysis of tungsten wire obtained from Thermionic Products Company, Plainfield, New Jersey.

Element	Content (%)
W	99.95
Ni	<0.002
Si	<0.005
Al	<0.005
Ca	<0.003
Mn	<0.003
Mg	<0.003
C	<0.004
Mo	<0.003

V. RESULTS

A representative set of results for ϵ, R_{44}, R_{28}, and R_{32} as functions of gas pressure and filament temperature is shown in Figs. 3 through 8. Figure 3 shows the dependence of ϵ on pressure at constant temperatures of 2160, 2290, 2540, 2785, and 2900°K. Figures 4 through 8 show the pressure dependence of R_{44}, R_{28}, and R_{32} at different temperatures. The curves are least-squares fits of the data. The pressure dependence of ϵ, R_{44}, and R_{28}, obtained from the least-squares fits, is summarized in Table II.

Table II. Pressure dependence of ϵ, R_{44}, and R_{28} at five temperatures.

	Values of x in ϵ, R_{44}, or $R_{28} = CP^x$					
	Low-pressure region			High-pressure region		
Temperature (°K)	ϵ	R_{44}	R_{28}	ϵ	R_{44}	R_{28}
2160	-0.05	0.95	0.75	-0.47	0.53	0.53
2290	+0.06	1.06	0.87	-0.46	0.54	0.51
2540	0.13	1.13	1.08	-0.29	0.72	0.69
2785	0.10	1.10	1.13	-0.05	0.95	0.92
2900	0.10	1.10	1.08	no noticeable change		

Reaction probabilities R_{44}, R_{28}, and R_{32} were determined on three different filaments, but the data shown in Figs. 3 through 8 are all from one filament. These data are shown because for this particular filament the widest range of gas pressure was used. A comparison of the results obtained with the three filaments is shown in Fig. 9. The curves are taken from Fig. 3, for filament 3; the points are for filaments 1 and 2. The agreement is within the scatter in the measurements. Comparable agreement is obtained for the R_{44}, R_{28}, and R_{32} curves.

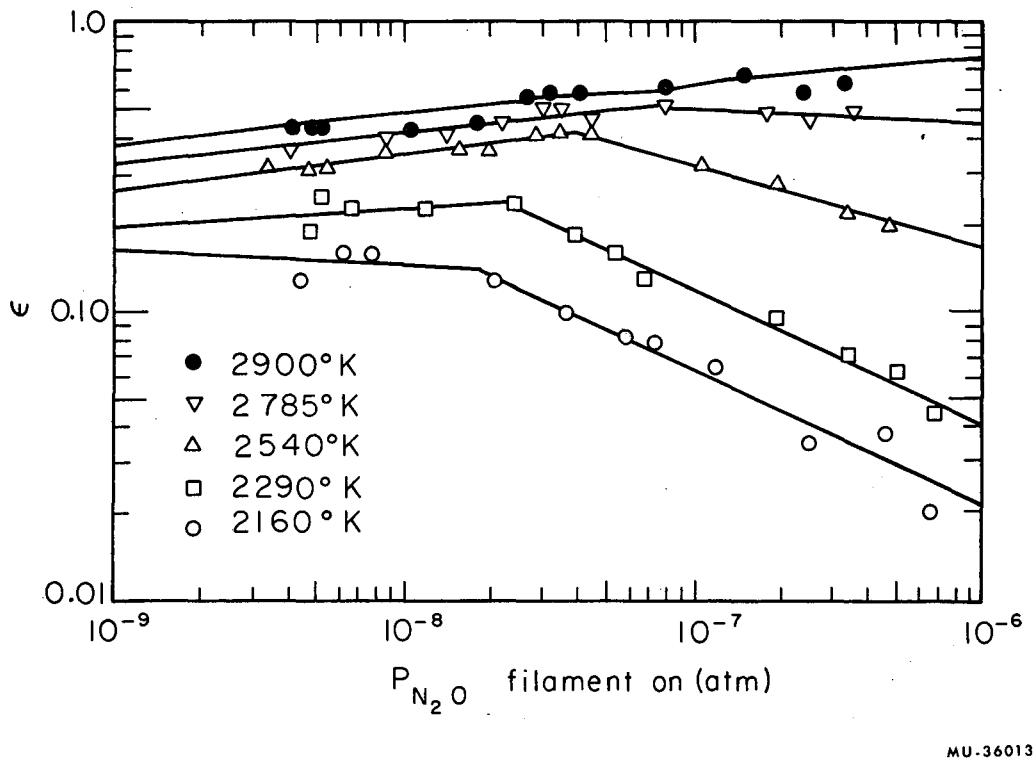

Fig. 3. Reaction probability as a function of N_2O pressure and filament temperature.

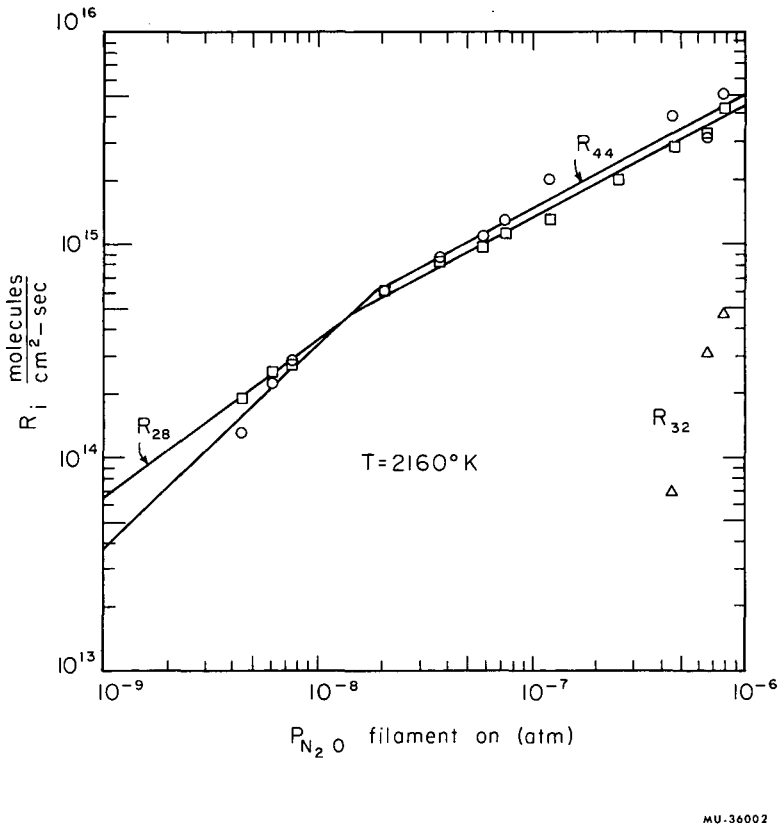

Fig. 4. R_{44}, R_{28}, and R_{32} as a function of N_2O pressure at 2160°K.

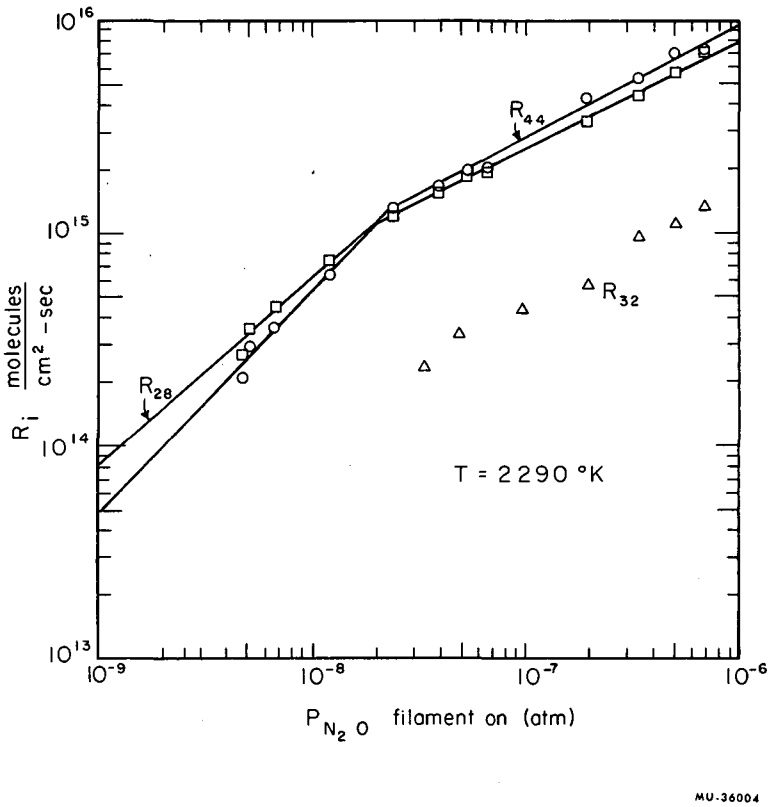

Fig. 5. R_{44}, R_{28}, and R_{32} as a function of N_2O pressure at 2290°K.

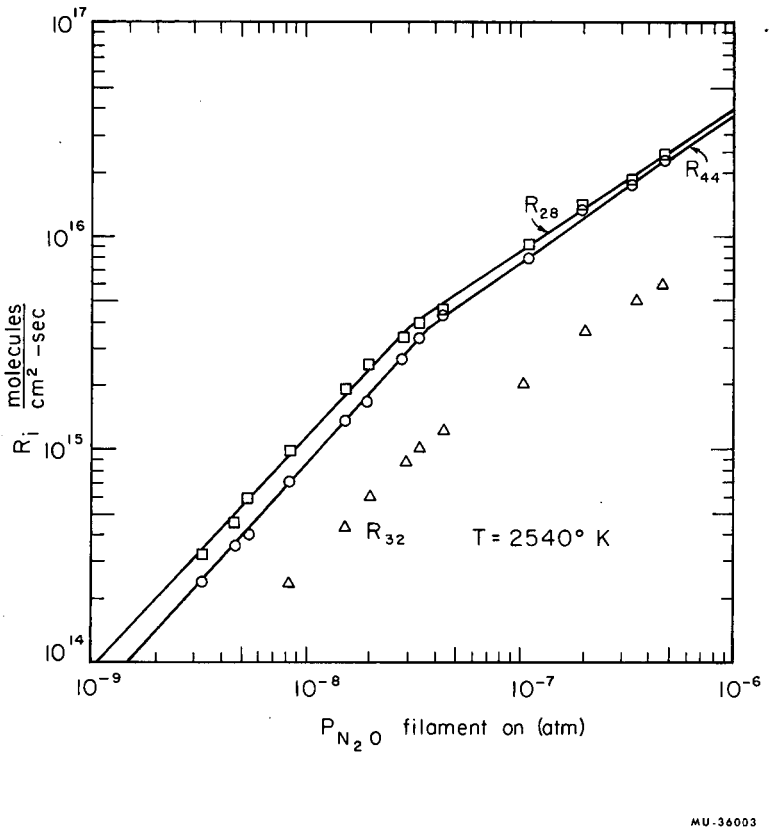

Fig. 6. R_{44}, R_{28}, and R_{32} as a function of N_2O pressure at 2540°K.

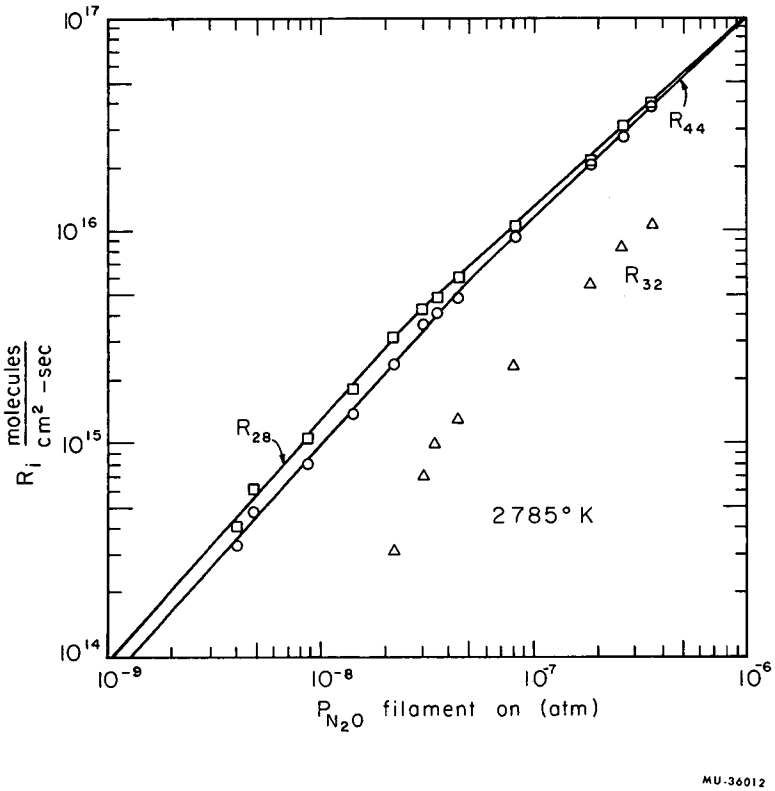

Fig. 7. R_{44}, R_{28}, and R_{32} as a function of N_2O pressure at 2785°K.

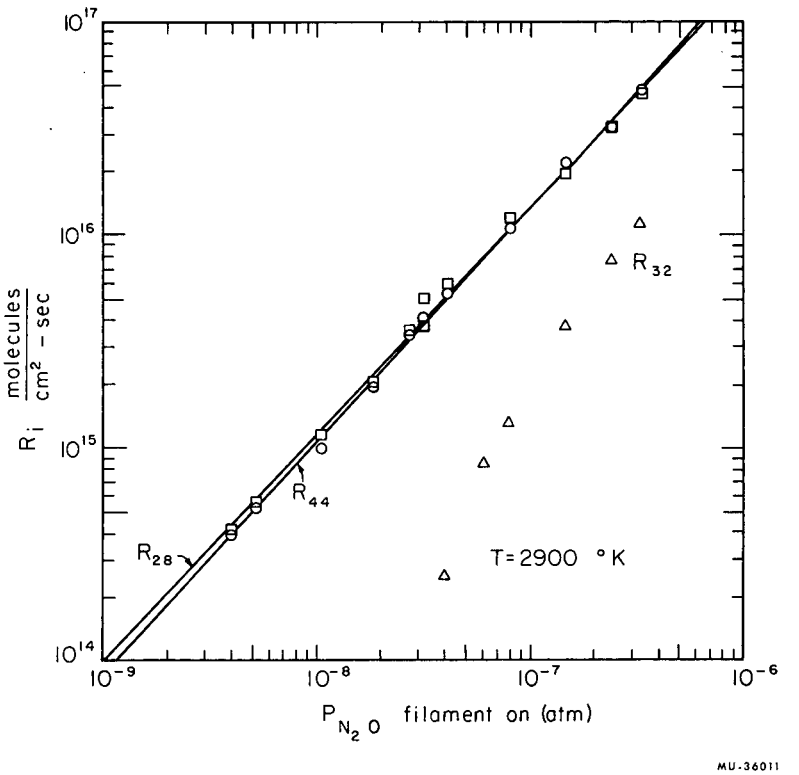

Fig. 8. R_{44}, R_{28}, and R_{32} as a function of N_2O pressure at 2900°K.

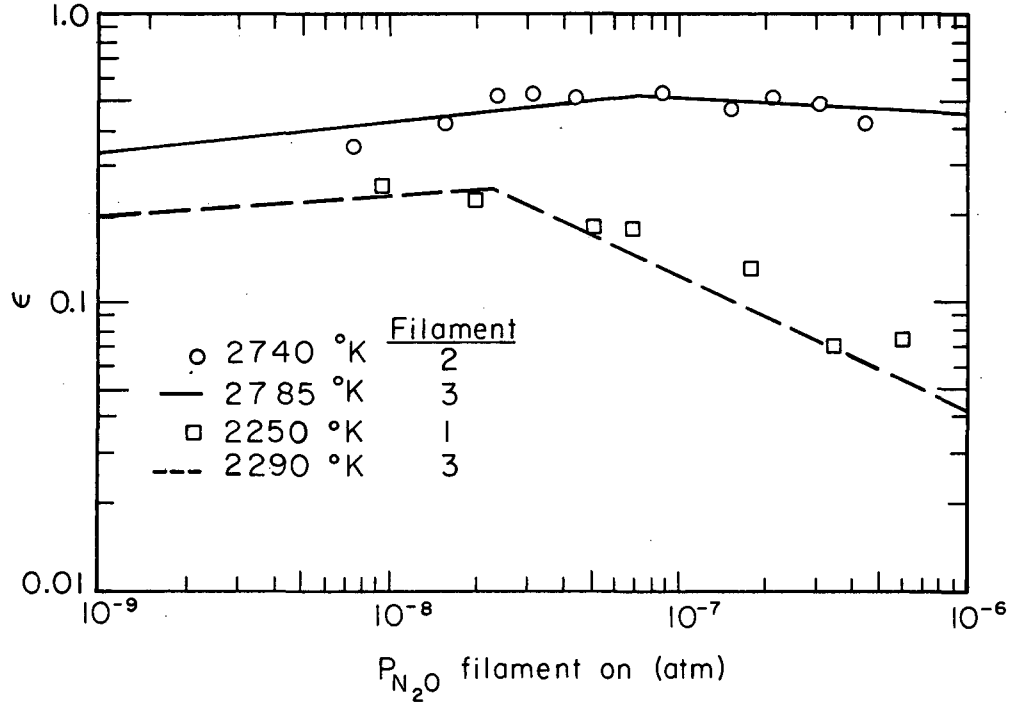

Fig. 9. Comparison of results obtained on three different filaments.

Figure 10 shows the dependence of R_w on gas pressure at constant temperature. The curves are least-squares fits of the data. The dependence of R_w at different temperatures on the nitrous oxide pressure is shown in Table III.

Table III. Pressure dependence of R_w at four temperatures.

T (°K)	Value of x in $R_w = C' P^x$
2220	0.85
2440	0.83
2550	0.87
2735	0.74

The data from which ϵ and all the rates were calculated are included in the Appendix.

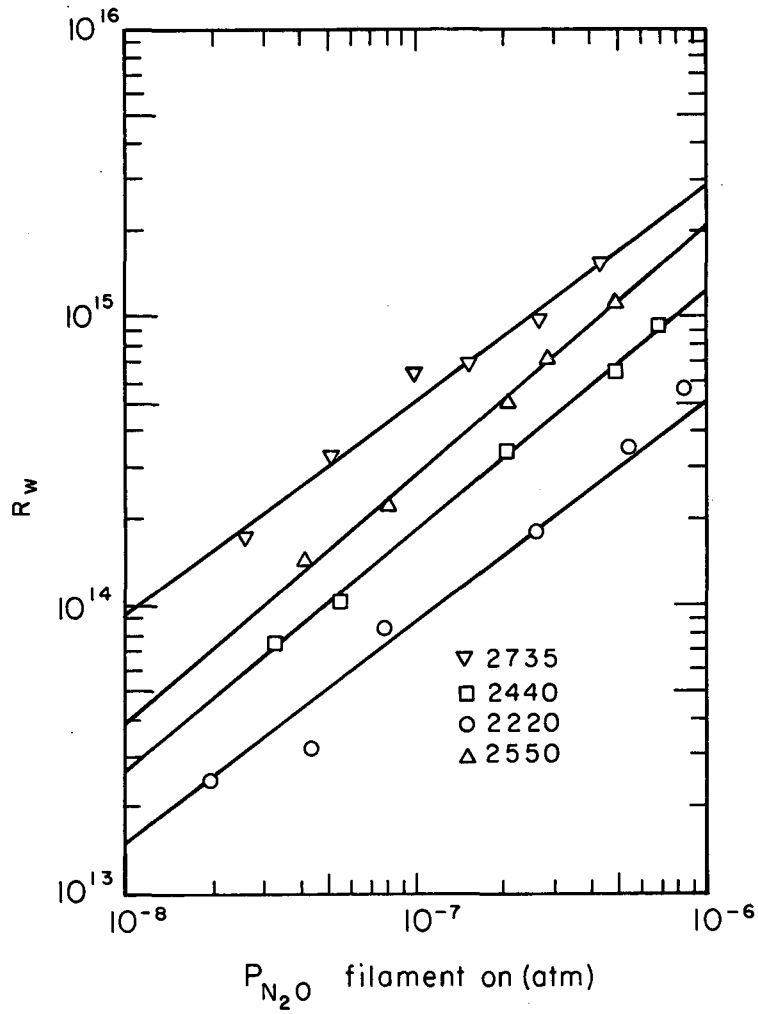

Fig. 10. R_w as a function of N_2O pressure at constant temperature.

VI. DISCUSSION OF RESULTS

A. Qualitative Description

The reaction probability ϵ for nitrous oxide is not equivalent to the sticking coefficient s, which is defined as that fraction of the total number of gas particles impinging on a surface that stick or become chemically adsorbed on that surface.[6] It will be seen later that some of the N_2O molecules react with chemisorbed oxygen atoms on the surface without becoming chemisorbed themselves. Thus the reaction probability will be larger than the sticking coefficient and cannot be expected to show the same temperature and pressure dependence as is usually shown by the sticking coefficient.

Several facts should be noted about the ϵ-pressure curves in Fig. 3. At the four lower temperatures there is a change in the slope of the curves, which occurs at increasing pressures as the temperature increases. The data are not precise enough to reveal a change in slope at 2900°K. Except at 2160°K, the slopes of the curves at low pressures are positive and at higher pressures are negative, with absolute values that decrease as the temperature increases. Over the entire experimental pressure range, ϵ increases with temperature, and the rate of increase with temperature is greater at 10^{-6} atm than at 10^{-9} atm.

Figures 4 through 8 show that within experimental scatter, the R_{44} and R_{28} curves are coincident. The value of R_{32} ranges from one-eighth to one-fifth the value of R_{44} or R_{28} and increases more rapidly with increasing temperature than do the values of R_{44} or R_{28}.

From this information and what is known about the mechanism of the decomposition of N_2O on platinum filaments and the chemisorption of oxygen and nitrogen on tungsten, we have deduced a possible mechanism for the tungsten-nitrous oxide reaction.

B. Deduction of a Possible Reaction Mechanism

Of the many investigations of the decomposition of N_2O on platinum filaments, only the most recent need be mentioned here. Riekert and Staib[7] studied the decomposition of N_2O on platinum filaments in the pressure range above 5 torr and at platinum temperatures from 500 to 1200°K. Lintz and Riekert[8] studied the effect of N_2O temperature (90 to 298°K) on its decomposition rate on platinum filaments at small constant N_2O pressures (under 10^{-4} torr) and platinum temperatures between 1200 and 1300°K. They proposed the following mechanism for the decomposition of N_2O on platinum filaments (#designates a site available for chemisorption and O-# designates a chemisorbed oxygen atom):

$$N_2O(g) + \# \rightarrow N_2(g) + O - \#$$
$$N_2O(g) + O - \# \rightarrow N_2(g) + O_2(g) + \#$$
$$2(O - \#) \rightarrow O_2(g) + 2(\#)$$
$$O_2(g) + 2(\#) \rightarrow 2(O - \#).$$

At N_2O pressures between 5×10^{-4} and 1×10^{-3} torr and a platinum filament at 1400°K, Mitani and Harano have shown that oxygen atoms evaporate from the platinum filament.[9] Thus the following step should be added to the reaction mechanism:

$$O - \# \rightarrow O(g) + \#.$$

For interpretation of the results of this investigation, the chemisorbed state is assumed to be preceded by a physisorbed precursor state that acts as a reservoir for the subsequent chemisorbed state which has a much higher binding energy. The concept of a physisorbed precursor state has been proposed by Lennard-Jones,[10] Rideal,[11] Becker and Hartman,[12] and Ehrlich.[13, 14] Ehrlich[13, 14] has discussed the kinetics and mechanism of chemisorption on metals

using this concept, and Smith[6] has derived equations for the sticking coefficients of nitrogen and carbon monoxide on tungsten by using a model involving a physisorbed precursor state. In discussing the low-pressure oxidation of niobium at 1500 to 2000°K, Kofstad and Espevik[15] assume that oxygen molecules first become physically adsorbed on the surface and that subsequent chemisorption occurs on specific surface sites from the reservoir of physically adsorbed molecules.

Lintz and Riekert found that, at the beginning of the decomposition reaction of N_2O on platinum, the collision yield of the reaction does not depend on the temperature of the gases.[8] It is possible that the first reaction in the above mechanism involves a precursor physiorbed state.

Redmond,[16] who investigated the decomposition of N_2O in the pressure range 0.02 to 4.0 torr on platinum heated from 820°K to 1090°K, found that added nitrogen and nitric oxide do not affect the decomposition reaction; on the other hand (as has been observed by others) added oxygen retarded the decomposition reaction, regardless of the source of the oxygen.

No studies of nitrous oxide decomposition on tungsten have been described in the literature, although many studies of the reaction of oxygen with tungsten have been reported. Becker and Brandes concluded that oxygen molecules striking a clean tungsten surface are physically adsorbed for a short time, during which they may evaporate as molecules or become adsorbed as atoms.[17] Oxygen chemisorbed as atoms also evaporates as atoms.[18]

Above 2100°K, $WO_2(g)$ has been shown by mass spectrometer to be the major species formed in the reaction of oxygen with tungsten.[19] At a tungsten temperature of 2800°K and a nitrogen pressure of 10^{-6} atm, Anderson has shown that the reaction rate of tungsten with nitrogen is negligible so that the formation of tungsten nitrides need not be considered in the reaction sequence.[20]

For the tungsten—nitrous oxide reaction, a possible first step is physical adsorption:

$$N_2O(g) \underset{k_2}{\overset{k_1}{\rightleftharpoons}} N_2O(p.a.) \qquad (2)$$

where (p. a.) refers to the physisorbed precursor state. In this state many reactions are possible. One set of reactions that satisfies the results obtained in this investigation is

$$N_2O(p.a.) + \# \xrightarrow{k_3} N_2(g) + O - \# \qquad (3)$$

$$N_2O(p.a.) + O - \# \xrightarrow{k_4} N_2(g) + \# + O_2(g) \qquad (4)$$

$$O - \# \xrightarrow{k_5} O(g) + \# \qquad (5)$$

$$2(O - \#) + W \xrightarrow{k_6} WO_2(g) + 2\#. \qquad (6)$$

Reaction 4 is probably necessary to account for the molecular oxygen observed as a reaction product, since O_2 is not a significant product of desorption of chemisorbed oxygen.

According to the reaction mechanism proposed above, nitrogen is not chemisorbed on tungsten so that the presence of excess nitrogen over the nitrous oxide should not significantly affect the reaction probability. A mixture of 10 parts nitrogen to 1 part nitrous oxide was passed through the reaction vessel and the reaction probability was determined at 2660°K. The results are compared with those for pure nitrous oxide in Fig. 11. As predicted from the mechanism, the excess of nitrogen over the nitrous oxide had no effect on the reaction probability.

The rate of generation of molecular oxygen, presumably by reaction (4), was only from one-eighth to one-fifth R_{44} instead of being always one-half R_{44}, as expected if reaction 4 accounted for all oxygen

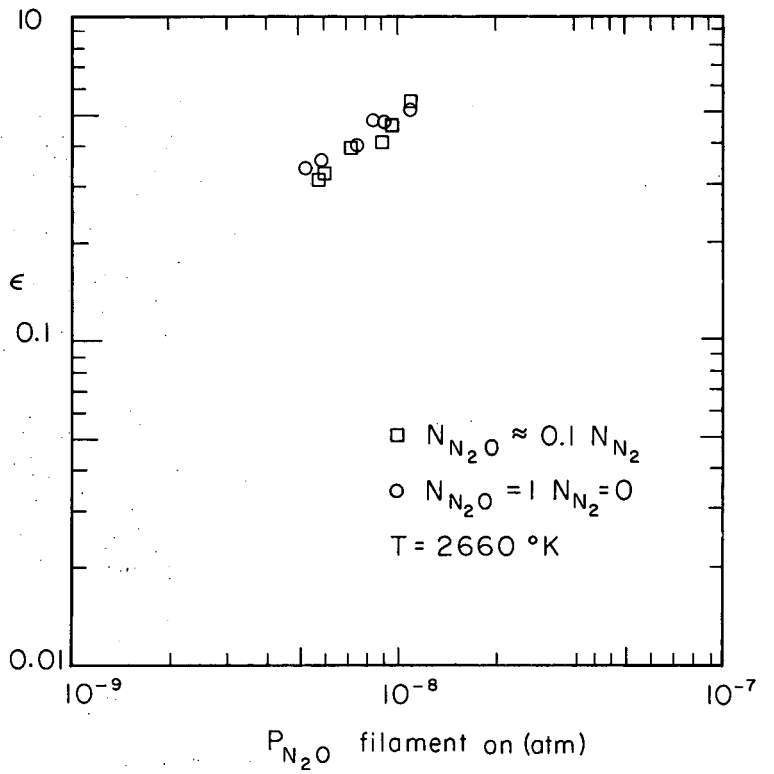

Fig. 11. Reaction probability as a function of N_2O pressure at 2660°K for mixtures of N_2 and N_2O.

from the nitrous oxide decomposition. However, the rate of O_2 generation varied with temperature and nitrous oxide pressure almost directly with the rate of nitrous oxide decomposition, except at 2160°K where the rates were lowest and therefore most difficult to measure accurately. The measured rate of WO_2 formation was too low to account for much of the discrepancy. Recent measurements by Schissel and Trulson indicate that oxygen-atom generation should vary more steeply with temperature than tungsten dioxide generation and should probably be comparable to tungsten oxide generation only at the highest temperatures.[21] Probably the value of measured O_2 generation is about one half the actual value. Efforts to improve the oxygen balance by more careful calibration were unsuccessful. Thus, if the available sites for chemisorption could be filled, the reaction probability should be greatly reduced. Pure nitrous oxide, as well as mixtures of oxygen and nitrous oxide in the ratios of 15.5 to 1, 2.3 to 1, were passed through the reaction vessel and the reaction probability of nitrous oxide was determined at 2550°K. The results are shown in Fig. 12. As predicted, the presence of gases that can fill the available sites for chemisorption decreases the reaction probability for nitrous oxide, the amount of decrease depending on the relative amounts of the two gases present.

According to the mechanism represented by Eqs. (1) to (6) above,

$$R_{44} = d[N_2O(g)]/dt = -k_1[N_2O(g)] + k_2[N_2O(p.a.)], \qquad (7)$$

where the square brackets denote concentration. Assuming a steady state for the precursor, i.e.,

$$\frac{d[N_2O(p.a.)]}{dt} \approx 0$$

we find that

$$[N_2O(p.a.)] = \frac{k_1[N_2O(g)]}{k_2 + k_3(1-\theta) + k_4\theta} \qquad (8)$$

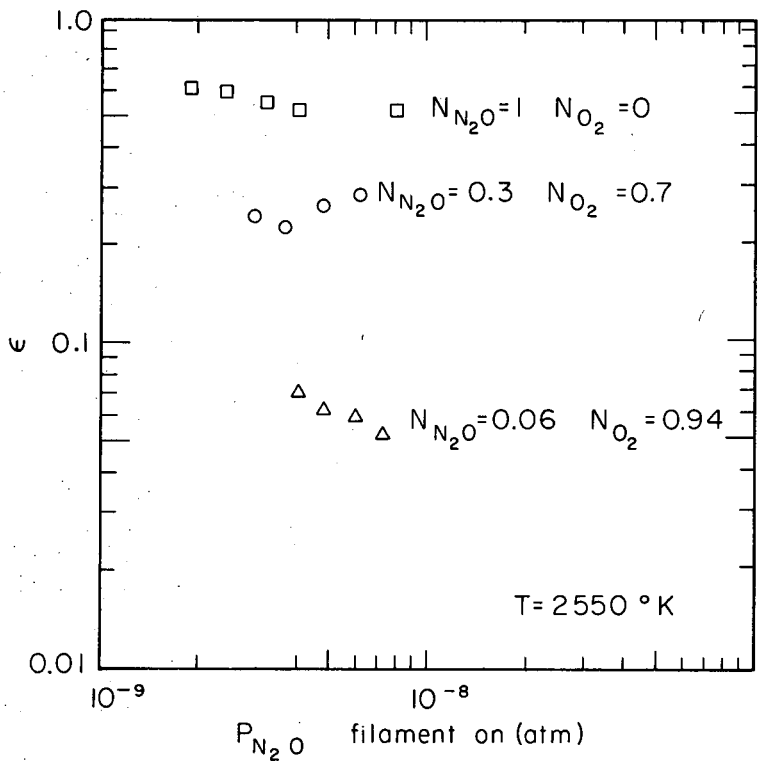

Fig. 12. Reaction probability as a function of N_2O pressure at 2550°K for mixtures of O_2 and N_2O.

and that

$$R_{44} = -k_1[N_2O(g)] \left\{1 - \frac{k_2}{k_2 + k_3(1-\theta) + k_4\theta}\right\}, \tag{9}$$

(where θ is the fraction of the surface covered), or

$$R_{44} = -k_1[N_2O(g)] \left\{\frac{k_3 + \theta(k_4 - k_3)}{k_2 + k_3 + \theta(k_4 - k_3)}\right\} \tag{10}$$

in which the bracketed quantity is the reaction probability.

Assuming a steady state for the chemisorbed oxygen, i.e.,

$$\frac{d\theta}{dt} = 0,$$

and neglecting reaction (6) because R_w is less than $0.1R_{44}$, we determine that the expression for the fractional surface coverage is

$$\theta = \frac{k_3}{k_3 + k_4 + \frac{k_5}{[N_2O(p.a.)]}}. \tag{11}$$

The pressure dependence of θ is in the term $k_5/[N_2O(p.a.)]$, which arises from desorption of oxygen atoms from the tungsten surface. Since $[N_2O(p.a.)]$ is proportional to the pressure, θ will also be proportional to the pressure, but the pressure dependence will be small because the rate of oxygen-atom desorption is small in the experimental range. As shown in Fig. 3 and Table II, ϵ increased very slightly with increasing pressure in the low-pressure range.

Equation (9) indicates that R_{44} should have a greater-than-first-power pressure dependence because of the pressure dependence of ϵ. The expected pressure dependence was observed experimentally as shown in Figs. 4 to 8 and Table II.

We assumed earlier that the precursor state is a two-dimensional gas physically adsorbed on the tungsten and that desorption will occur by a unimolecular evaporation reaction. However, as the concentration of physically adsorbed N_2O increases, desorption might also occur by a bimolecular reaction such as

$$N_2O(p.a.) + N_2O(p.a.) = 2N_2O(g) \qquad (12)$$

or

$$N_2O(p.a.) + N_2O(p.a.) = N_2O(g) + N_2O(p.a.). \qquad (13)$$

The rate of desorption for reaction (13) is

$$k_2'[N_2O(p.a.)]^2,$$

at at high pressures of N_2O may be large compared with either $k_3[N_2O(p.a.)](1-\theta)$ or $k_4[N_2O(p.a.)]\theta$, so that the rates of reactions (3) and (4) can be neglected in the steady-state treatment. The steady-state concentration then becomes

$$[N_2O(p.a.)] = (k_1/k_2')^{\frac{1}{2}}[N_2O(g)]^{\frac{1}{2}} \qquad (14)$$

and R_{44} becomes

$$R_{44} = -k_1[N_2O(g)] + (k_1k_2')^{\frac{1}{2}}[N_2O(g)]^{\frac{1}{2}}. \qquad (15)$$

The term $k_1[N_2O(g)]$ is proportional to P_{N_2O} and the term $(k_1k_2')^{\frac{1}{2}}[N_2O(p.a.)]^{\frac{1}{2}}$ is proportional to $(P_{N_2O})^{\frac{1}{2}}$. Thus, Eq. (15) shows that the pressure dependence of R_{44} (and of R_{28} and R_{32}) will be between $\frac{1}{2}$ and 1, as was experimentally observed.

As the tungsten temperature is increased, k_3 and k_4 increase so that the concentration of nitrous oxide in the precursor state decreases, as shown in Eq. (8). Therefore, the pressure at which

deviations from the first-power dependence on nitrous oxide pressure occurs will increase as the temperature increases, as we experimentally observed.

Bimolecular collisions in the precursor state may also affect the rate of chemisorption of oxygen atoms by reaction (3) and the rate of formation of molecular oxygen by reaction (4) of the proposed mechanism. Bimolecular collisions may result in deactivation of physically adsorbed nitrous oxide molecules, preventing them from reacting according to steps (3) and (4) in the mechanism. The deactivation will also cause a deviation from linearity in the overall reaction rate, and the pressure at which the deviation occurs will increase as the temperature is increased.

As shown by Eq. (9), the expression for the overall rate of the tungsten—nitrous oxide reaction involves many different rate constants. For this reason log R_{44} will not be plotted vs $1/T$, and an "apparent" activation energy for the overall reaction will not be calculated because it would be meaningless for such a complex reaction. For the same reason, empirical relationships will not be derived for the rate as a function of temperature and pressure. However, some estimates for the rate constants and activation energies are made in Sec. VI. D.

C. Formation of Tungsten Oxide

By defining

$$\epsilon' = (\tfrac{1}{2})\,(R_w/\nu_{44}), \tag{16}$$

where ϵ' is the probability that a nitrous oxide molecule that strikes the filament will be converted to a $WO_2(g)$ molecule and ν_{44} and R_w are defined as before, an indication of the oxidizing efficiency of the N_2O is obtained. The calculated values of ϵ' obtained by our taking

R_w from the least-squares fits of Fig. 10 are given in Table IV.

Table IV. Oxidizing efficiency of nitrous oxide.

T(°K)	Values of ϵ' at P_{N_2O}		
	10^{-8}	10^{-7}	10^{-6}
2220	0.0032	0.0019	0.0011
2440	0.0057	0.0039	0.0026
2550	0.0084	0.0060	0.0045
2735	0.020	0.011	0.0063

These data confirm that when a nitrous oxide molecule strikes a tungsten filament heated from 2000 to 3000°K the principal reaction is the decomposition of the nitrous oxide into molecular oxygen and nitrogen.

According to the reaction mechanism, $WO_2(g)$ is formed by the reaction

$$W + 2(O - \#) \xrightarrow{k_6} WO_2(g) + 2\#. \qquad (17)$$

Since the actual removal of tungsten atoms is presumably by an elementary reaction, a plot of log R_w vs 1/T is meaningful. Figure 13 is such a plot at $P_{N_2O} = 10^{-8}$, 10^{-7}, and 10^{-6} atm, the values for R_w being taken from the least-squares fits of Fig. 10. Straight lines are drawn through the points at all three pressures that have the same slope of 41 500 cal/mole. The increase in R_w with pressure is caused by the increased surface coverage at the higher pressures.

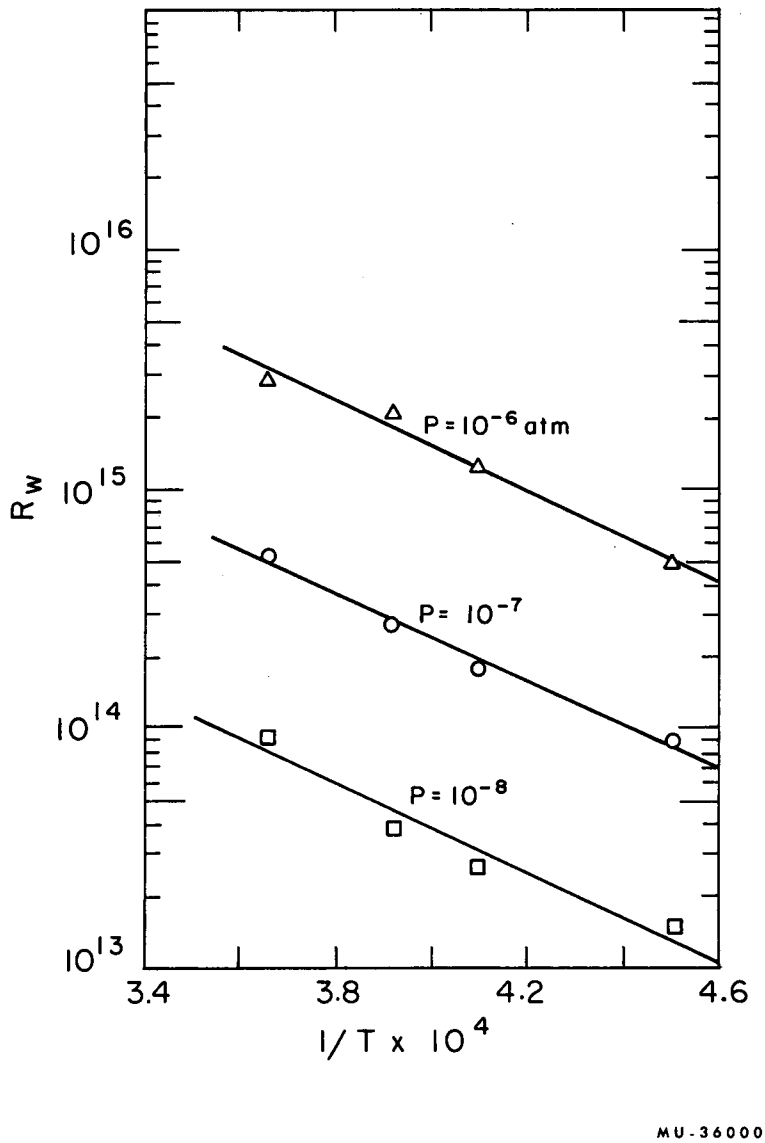

Fig. 13. R_w as a function of 1/T at P_{N_2O} = 10^{-8}, 10^{-7}, and 10^{-6} atm.

D. Estimation of Rate Constants and Activation Energies

From Eq. (10) it is seen that

$$\epsilon = \frac{k_3 + \theta(k_4 - k_3)}{k_2 + k_3 + \theta(k_4 - k_3)} , \tag{18}$$

and for $\theta = 0$ it follows that

$$\epsilon = \frac{k_3}{k_2 + k_3} \tag{19}$$

and that

$$\frac{k_3}{k_2} = \frac{\epsilon}{1 - \epsilon} . \tag{20}$$

According to Ehrlich's treatment,[13]

$$k_3 = K_3 \nu_3 e^{-E_3/kT} \tag{21}$$

and

$$k_2 = K_2 \nu_2 e^{-E_2/kT} , \tag{22}$$

where K_3 and K_2 are probability factors for reaction and desorption, respectively; ν_3 and ν_2 are identical and are the frequency of vibration of the physically adsorbed N_2O molecules perpendicular to the surface; and E_3 and E_2 are activation energies. From Eqs. (21) and (22) it follows that

$$\frac{k_3}{k_2} = \frac{K_3 e^{-E_3/kT}}{K_2 e^{-E_2/kT}} . \tag{23}$$

From the work of Meyer and Gomer[22] and De Poorter and Searcy[23] it is reasonable to assume (a) that the physically adsorbed N_2O is not at the same temperature as the tungsten filament and (b) that the average temperature of the physically adsorbed N_2O is independent of the temperature of the tungsten filament. From the results in reference 23, a reasonable estimate of the maximum temperature of the physically adsorbed N_2O is 1050°K. Because the average temperature of the physically adsorbed layer is independent of the tungsten temperature, the term $e^{-E_2/kT}$ in Eq. (23) will be constant and

$$\frac{k_3}{k_2} = (\text{const})\, e^{-E_3/kT} \tag{24}$$

so that a plot of $\epsilon/(1-\epsilon)$ vs $1/T$ at $\theta = 0$ will have a slope of E_3/k.

Figure 14 is a plot of $\epsilon/(1-\epsilon)$ vs $1/T$ for a N_2O pressure of 10^{-9} atmospheres. Although at this pressure θ is probably not zero, it will be small. As seen from the figure, a straight line is obtained. The value for E_3 calculated from the slope of the line is 19 000 cal/mole.

An upper limit on E_2, the heat of physical adsorption, is 10 000 cal/mole. The vibration frequency ν_2 is probably between 10^{12} and 10^{14} sec^{-1}, and a value of 10^{13} sec^{-1} is assumed. Then

$$k_2 = 10^{13}\, e^{-10\,000/RT}, \tag{25}$$

and at 1050°K

$$k_2 = 8.3 \times 10^{10}\ sec^{-1}.$$

The time of physical adsorption will be $1/k_2$ or about 1×10^{-11} sec.

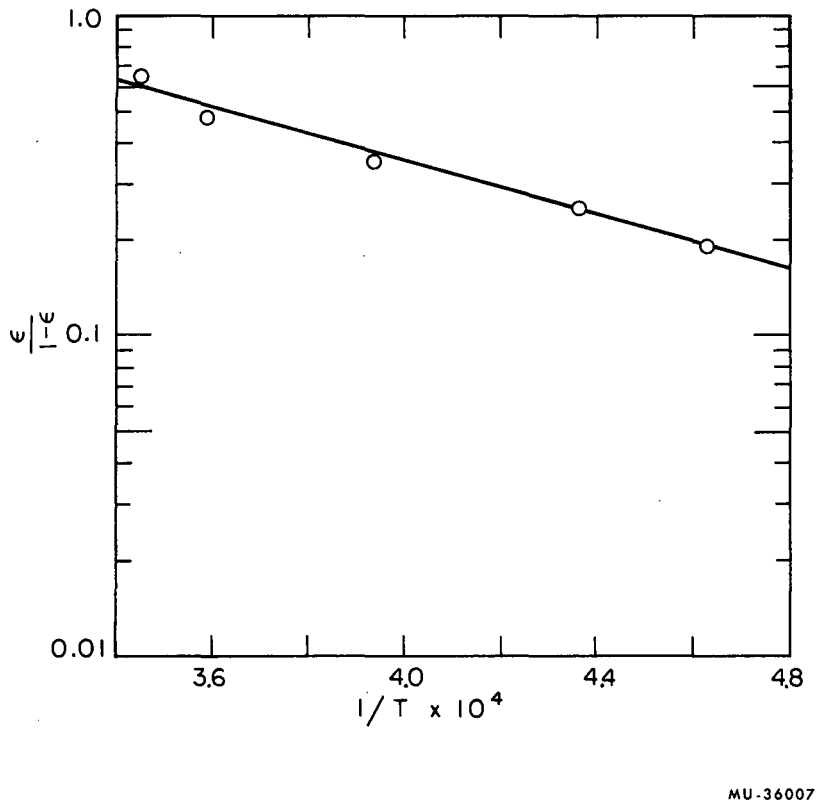

Fig. 14. $\frac{\epsilon}{1-\epsilon}$ as a function of 1/T at $P_{N_2O} = 10^{-9}$ atm.

Using the activation energy obtained from Fig. 14 and the same estimated value for the vibration frequency, we obtain

$$k_3 = 10^{13} e^{-19\,000/RT}. \qquad (26)$$

At 2160°K, k_3 calculated from Eq. (26) is 10^{11} sec^{-1}, and at 2900°K, k_3 is 4×10^{11} sec^{-1}.

By means of the rate constants calculated from Eqs. (25) and (26), ϵ can be calculated from Eq. (18), again with the assumption that θ is zero. The calculated value at 2160°K is 0.55 and at 2900°K is 0.83. The experimental values at a N_2O pressure of 10^{-9} atmospheres and at temperatures of 2160 and 2900°K are 0.16 and 0.39 respectively.

DeBoer estimates the activation energy for surface diffusion to be about one-half the heat of adsorption.[24] On the basis of this estimate, the rate constant for diffusion will be

$$k_D = 10^{13} e^{-5\,000/RT} sec^{-1}, \qquad (27)$$

and at 1050°K will have a numerical value of 9×10^{11} sec^{-1}. From this calculation the rate of surface diffusion in the precursor state is shown to be about ten times the rate of evaporation by the unimolecular evaporation reaction. At 2160°K the rate of surface diffusion in the precursor state is also ten times the rate of reaction, by steps 3 and 4 in the mechanism. However, at 2900°K the rate of reaction (3) is almost half the diffusion rate, and if the rate of reaction (4) is taken into account, the rate of reaction from the precursor state may be about the same as the rate of surface diffusion. These circumstances are consistent with the suggestion made earlier that at low temperatures and high pressures desorption by a bimolecular reaction may become important relative to desorption by a unimolecular reaction. In the high-pressure range at 2900°K, desorption by the bimolecular reaction is not likely to occur because the physically adsorbed N_2O

molecules will react with the surface before they collide with each other. In the high-pressure—low-temperature range there will be many chances for collision before the N_2O molecules evaporate or react with the surface.

Unfortunately, neither k_4 nor the activation energy for k_4, can be determined. Because the surface coverage is a function of k_3, k_4, and k_5, the activation energy for k_4 cannot be determined from a plot of R_{32} vs $1/T$.

The rate constant and activation energy for the evaporation of atomic oxygen has been determined by Johnson and Vick[25] and is given by

$$k_5 = 5\times10^{28} \exp(-144\,000/RT)\ \text{cm}^{-2}\text{-sec}^{-1}.$$

VII. SUMMARY

The high-temperature—low-pressure reaction between nitrous oxide and tungsten is mainly a decomposition reaction that is unaffected by excess nitrogen but greatly retarded by excess oxygen. About one in a thousand nitrous oxide molecules that strike the surface reacts to form $WO_2(g)$ at a tungsten temperature of 2220°K and a nitrous oxide pressure of 10^{-6} atm, whereas at 2735°K and 10^{-8} atm, one in fifty nitrous oxide molecules that strike the surface are converted to $WO_2(g)$. The results of this investigation are consistent with a six-step reaction mechanism involving:

(1) Physical adsorption of the nitrous oxide,

(2) Partial evaporation of the physically adsorbed nitrous oxide,

(3) Decomposition of the physically adsorbed nitrous oxide molecules into nitrogen gas and chemisorbed oxygen atoms,

(4) Reaction of the physically adsorbed nitrous oxide molecules with chemisorbed oxygen atoms, producing molecular nitrogen and oxygen,

(5) Evaporation of the chemisorbed oxygen atoms, and

(6) Reaction of two chemisorbed oxygen atoms with the tungsten giving $WO_2(g)$.

The decomposition rate of N_2O and the rate of formation of WO_2 both increase with increasing temperature and pressure.

ACKNOWLEDGMENTS

The author expresses his sincere appreciation to Professor Alan W. Searcy for his guidance and direction, to Dr. David J. Meschi for his many helpful suggestions, to the Corning Glass Works for a fellowship for the 1962-63 academic year, and to the many others who gave many helpful hints and helped with the construction of the apparatus.

This work was performed under the auspices of the U. S. Atomic Energy Commission.

APPENDIX

Tables of Experimental Data

Table V. Experimental data for tungsten–nitrous oxide reaction at 2160°K.

P_{44} with filament cold	P_{44}	P_{28}	P_{32}	ϵ	R_{44}	R_{28}	R_{32}
6.06×10^{-9}	4.39×10^{-9}	2.55×10^{-9}		0.13	1.33×10^{14}	1.93×10^{14}	
8.90×10^{-9}	6.06×10^{-9}	3.40×10^{-9}		0.16	2.24×10^{14}	2.57×10^{14}	
1.12×10^{-8}	7.61×10^{-9}	3.65×10^{-9}		0.16	2.83×10^{14}	2.76×10^{14}	
2.84×10^{-8}	2.06×10^{-8}	8.20×10^{-9}		0.13	6.23×10^{14}	6.20×10^{14}	
4.44×10^{-8}	3.68×10^{-8}	1.1×10^{-8}		0.10	8.53×10^{14}	8.32×10^{14}	
7.22×10^{-8}	5.81×10^{-8}	1.3×10^{-8}		0.083	1.12×10^{15}	9.83×10^{14}	
9.03×10^{-8}	7.55×10^{-8}	1.5×10^{-8}		0.078	1.33×10^{15}	1.13×10^{15}	
1.43×10^{-7}	1.40×10^{-7}	1.7×10^{-8}		0.066	1.83×10^{15}	1.29×10^{15}	
2.77×10^{-7}	2.52×10^{-7}	2.7×10^{-8}		0.035	2.04×10^{15}	2.04×10^{15}	
5.16×10^{-7}	4.64×10^{-7}	3.8×10^{-8}	9.58×10^{-10}	0.038	4.09×10^{15}	2.87×10^{15}	6.93×10^{13}
7.10×10^{-7}	6.71×10^{-7}	4.3×10^{-8}	4.22×10^{-9}	0.020	3.11×10^{15}	3.25×10^{15}	3.06×10^{14}
8.51×10^{-7}	7.87×10^{-7}	5.8×10^{-8}	6.55×10^{-9}	0.028	5.11×10^{15}	4.38×10^{15}	4.74×10^{14}

Table VI. Experimental data for tungsten–nitrous oxide reaction at 2290°K.

P_{44} with filament cold	P_{44}	P_{28}	P_{32}	ϵ	R_{44}	R_{28}	R_{32}
7.35×10^{-9}	4.71×10^{-9}	3.6×10^{-9}		0.19	2.08×10^{14}	2.72×10^{14}	
8.90×10^{-9}	5.10×10^{-9}	4.7×10^{-9}		0.25	2.95×10^{14}	3.55×10^{14}	
1.12×10^{-8}	6.71×10^{-9}	5.9×10^{-9}		0.23	3.57×10^{14}	4.46×10^{14}	
1.97×10^{-8}	1.19×10^{-8}	9.8×10^{-9}		0.23	6.33×10^{14}	7.41×10^{14}	
4.10×10^{-8}	2.39×10^{-8}	1.62×10^{-8}		0.24	1.33×10^{15}	1.22×10^{15}	
6.06×10^{-8}	3.87×10^{-8}	2.05×10^{-8}		0.19	1.70×10^{15}	1.55×10^{15}	
8.00×10^{-8}	5.42×10^{-8}	2.50×10^{-8}		0.16	2.01×10^{15}	1.89×10^{15}	
9.29×10^{-8}	6.71×10^{-8}	2.60×10^{-8}		0.13	2.03×10^{15}	1.97×10^{15}	
2.48×10^{-7}	1.94×10^{-7}	4.40×10^{-8}	7.81×10^{-9}	0.095	4.27×10^{15}	3.33×10^{15}	5.66×10^{14}
4.13×10^{-7}	3.42×10^{-7}	5.80×10^{-8}	1.32×10^{-8}	0.070	5.55×10^{15}	4.38×10^{15}	9.58×10^{14}
5.93×10^{-7}	5.03×10^{-7}	7.50×10^{-8}	1.50×10^{-8}	0.061	7.12×10^{15}	5.67×10^{15}	1.09×10^{15}
7.74×10^{-7}	6.84×10^{-7}	9.3×10^{-8}	1.80×10^{-8}	0.045	7.13×10^{15}	7.03×10^{15}	1.31×10^{15}
5.16×10^{-8}	3.35×10^{-8}		3.21×10^{-9}				2.33×10^{14}
7.35×10^{-8}	4.90×10^{-8}		4.60×10^{-9}				3.33×10^{14}
1.34×10^{-7}	9.68×10^{-8}		5.92×10^{-9}				4.28×10^{14}

Table VII. Experimental data for tungsten–nitrous oxide reaction at 2540°K.

P_{44} with filament cold	P_{44}	P_{28}	P_{32}	ϵ	R_{44}	R_{28}	R_{32}
6.32×10^{-9}	3.29×10^{-9}	4.4×10^{-9}		0.31	2.36×10^{14}	3.33×10^{14}	
9.16×10^{-9}	4.71×10^{-9}	5.95×10^{-9}		0.32	3.50×10^{14}	4.50×10^{14}	
1.03×10^{-8}	5.35×10^{-9}	7.80×10^{-9}		0.32	3.97×10^{14}	5.90×10^{14}	
1.75×10^{-8}	8.51×10^{-9}	1.3×10^{-8}	3.21×10^{-9}	0.36	7.11×10^{14}	9.83×10^{14}	2.33×10^{14}
3.26×10^{-8}	1.56×10^{-8}	2.5×10^{-8}	5.92×10^{-9}	0.37	1.34×10^{15}	1.89×10^{15}	4.28×10^{14}
4.13×10^{-8}	1.97×10^{-8}	3.3×10^{-8}	8.32×10^{-9}	0.37	1.69×10^{15}	2.49×10^{15}	6.02×10^{14}
6.32×10^{-8}	2.86×10^{-8}	4.4×10^{-8}	1.18×10^{-8}	0.41	2.72×10^{15}	3.33×10^{15}	8.58×10^{14}
7.61×10^{-8}	3.42×10^{-8}	5.2×10^{-8}	1.39×10^{-8}	0.42	3.33×10^{15}	3.93×10^{15}	1.00×10^{15}
9.68×10^{-8}	4.41×10^{-8}	6.0×10^{-8}	1.70×10^{-8}	0.41	4.19×10^{15}	4.54×10^{15}	1.23×10^{15}
2.04×10^{-7}	1.06×10^{-7}	1.2×10^{-7}	2.77×10^{-8}	0.32	7.84×10^{15}	9.07×10^{15}	2.00×10^{15}
3.61×10^{-7}	1.97×10^{-7}	1.85×10^{-7}	4.91×10^{-8}	0.28	1.28×10^{16}	1.40×10^{16}	3.55×10^{15}
5.68×10^{-7}	3.42×10^{-7}	2.45×10^{-7}	6.87×10^{-8}	0.22	1.74×10^{16}	1.85×10^{16}	4.96×10^{15}
7.61×10^{-7}	4.84×10^{-7}	3.15×10^{-7}	8.06×10^{-8}	0.20	2.24×10^{16}	2.38×10^{16}	5.83×10^{15}

Table VIII. Experimental data for tungsten—nitrous oxide reaction at 2785°K.

P_{44} with filament cold	P_{44}	P_{28}	P_{32}	ϵ	R_{44}	R_{28}	R_{32}
8.26×10^{-9}	4.0×10^{-9}	5.5×10^{-9}		0.36	3.34×10^{14}	4.16×10^{14}	
1.08×10^{-8}	4.77×10^{-9}	8.1×10^{-9}		0.43	4.76×10^{14}	6.12×10^{14}	
1.88×10^{-8}	8.64×10^{-9}	1.4×10^{-8}		0.40	8.02×10^{14}	1.06×10^{15}	
3.15×10^{-8}	1.42×10^{-8}	2.35×10^{-8}		0.41	1.35×10^{15}	1.78×10^{15}	
5.10×10^{-8}	2.17×10^{-8}	4.20×10^{-8}	4.28×10^{-9}	0.46	2.31×10^{15}	3.17×10^{15}	3.10×10^{14}
7.47×10^{-8}	3.01×10^{-8}	5.70×10^{-8}	9.83×10^{-9}	0.51	3.56×10^{15}	4.31×10^{15}	7.12×10^{14}
8.64×10^{-8}	3.48×10^{-8}	6.40×10^{-8}	1.36×10^{-8}	0.50	4.04×10^{15}	4.84×10^{15}	9.85×10^{14}
1.05×10^{-7}	4.39×10^{-8}	8.0×10^{-8}	1.78×10^{-8}	0.47	4.79×10^{15}	6.05×10^{15}	1.29×10^{15}
1.99×10^{-7}	8.0×10^{-8}	1.4×10^{-7}	3.15×10^{-8}	0.51	9.47×10^{15}	1.06×10^{16}	2.28×10^{15}
4.39×10^{-7}	1.81×10^{-7}	2.85×10^{-7}	7.56×10^{-8}	0.49	2.05×10^{16}	2.15×10^{16}	5.47×10^{15}
6.06×10^{-7}	2.58×10^{-7}	4.2×10^{-7}	1.13×10^{-7}	0.46	2.75×10^{16}	3.17×10^{16}	8.22×10^{15}
8.51×10^{-7}	3.51×10^{-7}	5.3×10^{-7}	1.45×10^{-7}	0.49	3.99×10^{16}	4.01×10^{16}	1.05×10^{16}

Table IX. Experimental data for tungsten—nitrous oxide reaction at 2900°K.

P_{44} with filament cold	P_{44}	P_{28}	P_{32}	ϵ	R_{44}	R_{28}	R_{32}
9.03×10^{-9}	4×10^{-9}	5.5×10^{-9}		0.43	3.99×10^{14}	4.16×10^{14}	
1.16×10^{-8}	5.16×10^{-9}	7.0×10^{-9}		0.43	5.15×10^{14}	5.29×10^{14}	
2.32×10^{-8}	1.04×10^{-8}	1.5×10^{-8}		0.42	1.02×10^{15}	1.13×10^{15}	
4.39×10^{-8}	1.86×10^{-8}	2.70×10^{-8}		0.46	1.99×10^{15}	2.04×10^{15}	
7.10×10^{-8}	2.71×10^{-8}	4.70×10^{-8}		0.55	3.46×10^{15}	3.55×10^{15}	
8.51×10^{-8}	3.23×10^{-8}	6.6×10^{-8}		0.56	4.19×10^{15}	4.99×10^{15}	
1.08×10^{-7}	4.06×10^{-8}	7.6×10^{-8}	3.47×10^{-9}	0.57	5.38×10^{15}	5.75×10^{15}	2.51×10^{14}
2.19×10^{-7}	8.00×10^{-8}	1.6×10^{-7}	1.83×10^{-8}	0.59	1.10×10^{16}	1.21×10^{16}	1.32×10^{15}
4.26×10^{-7}	1.48×10^{-7}	2.6×10^{-7}	5.17×10^{-8}	0.64	2.21×10^{16}	1.97×10^{16}	3.74×10^{15}
6.45×10^{-7}	2.39×10^{-7}	4.3×10^{-7}	1.06×10^{-7}	0.58	3.21×10^{16}	3.25×10^{16}	7.66×10^{15}
9.29×10^{-7}	3.29×10^{-7}	6.0×10^{-7}	1.58×10^{-7}	0.62	4.73×10^{16}	4.54×10^{16}	1.14×10^{16}
1.68×10^{-7}	6.06×10^{-8}		1.20×10^{-8}				8.67×10^{14}

Table X. Experimental data for N_2-N_2O gas mixture experiments.

N_2-N_2O mixture			N_2O only		
P_{44} filament cold	P_{44}	ϵ	P_{44} filament cold	P_{44}	ϵ
8.1×10^{-9}	5.68×10^{-9}	0.32	7.8×10^{-9}	5.29×10^{-9}	0.34
8.6×10^{-9}	5.93×10^{-9}	0.33	9.0×10^{-9}	5.93×10^{-9}	0.36
1.15×10^{-8}	7.22×10^{-9}	0.39	1.2×10^{-8}	7.48×10^{-9}	0.40
1.45×10^{-8}	8.82×10^{-9}	0.42	1.5×10^{-8}	8.51×10^{-9}	0.48
1.675×10^{-8}	9.55×10^{-9}	0.47	1.62×10^{-8}	9.29×10^{-9}	0.47
2.10×10^{-8}	1.10×10^{-8}	0.54	2.05×10^{-8}	1.10×10^{-8}	0.52

Table XI. Experimental data for O_2-N_2O gas-mixture experiments.

n_{N_2O}	n_{O_2}	P_{44} filament cold	P_{44}	ϵ
0.06	0.94	4.75×10^{-9}	4.0×10^{-9}	0.071
0.06	0.94	5.75×10^{-9}	4.9×10^{-9}	0.064
0.06	0.94	7.0×10^{-9}	6.0×10^{-9}	0.060
0.06	0.94	8.4×10^{-9}	7.4×10^{-9}	0.053
0.3	0.7	4.9×10^{-9}	2.95×10^{-9}	0.25
0.3	0.7	6.0×10^{-9}	3.7×10^{-9}	0.23
0.3	0.7	8.4×10^{-9}	4.9×10^{-9}	0.27
0.3	0.7	1.1×10^{-8}	6.22×10^{-9}	0.29
1	0	4.9×10^{-9}	1.85×10^{-9}	0.62
1	0	6.22×10^{-9}	2.40×10^{-9}	0.60
1	0	7.98×10^{-9}	3.20×10^{-9}	0.56
1	0	9.61×10^{-9}	4.0×10^{-9}	0.53
1	0	1.94×10^{-8}	7.98×10^{-9}	0.53

n means mole fraction

Table XII. Experimental data for R_w determinations.

T (°K)	P_{44}	R_w
2220	8.41×10^{-7}	5.7×10^{14}
	5.47×10^{-7}	3.56×10^{14}
	2.61×10^{-7}	1.80×10^{14}
	7.81×10^{-8}	8.32×10^{13}
	4.37×10^{-8}	3.19×10^{13}
	1.96×10^{-8}	2.54×10^{13}
2440	6.85×10^{-7}	9.45×10^{14}
	4.93×10^{-7}	6.50×10^{14}
	2.01×10^{-7}	3.35×10^{14}
	5.56×10^{-8}	1.04×10^{14}
	3.24×10^{-8}	7.52×10^{13}
2550	4.9×10^{-7}	1.13×10^{15}
	2.85×10^{-7}	7.35×10^{14}
	2.1×10^{-7}	5.03×10^{14}
	8.2×10^{-8}	2.22×10^{14}
	4.2×10^{-8}	1.41×10^{14}
2735	4.26×10^{-7}	1.52×10^{15}
	2.65×10^{-7}	9.85×10^{14}
	1.55×10^{-7}	6.88×10^{14}
	9.98×10^{-8}	6.26×10^{14}
	5.03×10^{-8}	3.20×10^{14}
	2.52×10^{-8}	1.71×10^{14}

REFERENCES

1. S. Dushman, Vacuum Technique (John Wiley & Sons, Inc., New York, 1961), 2nd ed.
2. H. U. Anderson, Rev. Sci. Instr. 34, 703 (1963).
3. H. U. Anderson, Kinetic Studies of Reactions Occurring Between Tungsten and Gases at Low Temperatures and High Pressures (Ph. D. Thesis), UCRL-10135, April 1962 (unpublished), p. 42.
4. H. A. Jones and I. Langmuir, Gen. Elec. Rev. 30, 310, 354, 408 (1927).
5. H. U. Anderson, ibid, p. 15-21.
6. T. Smith, J. Chem. Phys. 40, 1805 (1964).
7. L. Riekert and M. Staib, Z. Elektrochem. 67, 976 (1963).
8. H. G. Lintz and L. Riekert, Z. Phys. Chemie-Neu Folge 42, 87 (1964).
9. K. Mitani and Y. Harano, Bull. Chem. Soc. Japan 32, 1386 (1959).
10. J. E. Lennard-Jones, Trans. Faraday Soc. 28, 333 (1932).
11. E. K. Rideal, Proc. Cambridge Phil. Soc. 35, 130 (1939).
12. J. A. Becker and C. D. Hartman, J. Phys. Chem. 57, 153 (1953).
13. G. Ehrlich, J. Phys. Chem. 59, 473 (1955).
14. G. Ehrlich, J. Phys. Chem. Solids 1, 1 (1956).
15. Per Kofstad and S. Espevik, J. Electrochem. Soc. 112, 153 (1965).
16. J. P. Redmond, J. Phys. Chem. 67, 788 (1963).
17. J. A. Becker and R. G. Brandes, J. Chem. Phys. 23, 1323 (1955).
18. G. Ehrlich, in Structure and Properties of Thin Films, edited by C. A. Neugebauer, J. B. Newkirk, and D. A. Vermilyea, (John Wiley, New York, 1959).
19. J. B. Berkowitz-Mattuck, A. Buchler, J. L. Engelke, and S. N. Goldstein, J. Chem. Phys. 39, 2722 (1963).
20. H. U. Anderson, ibid, p. 87.
21. P. O. Schissel and O. C. Trulson, Mass Spectrometric Investigation of the Oxidation of Tungsten, Union Carbide Research Institute, Technical Report No. C-26 (1964).

22. L. Meyer and R. Gomer, J. Chem. Phys. 28, 617 (1958).
23. G. L. De Poorter and A. W. Searcy, J. Chem. Phys. 39, 925 (1963).
24. J. H. deBoer, The Dynamical Character of Adsorption, (Clarendon Press, Oxford, 1953).
25. M. C. Johnson and F. A. Vick, Proc. Roy. Soc. (London), A151, 308 (1935).